Molecular Therapy
Methods & Clinical Development
Original Article

AAVrh10 Vector Corrects Disease Pathology in MPS IIIA Mice and Achieves Widespread Distribution of SGSH in Large Animal Brains

Michaël Hocquemiller,[1,6] Kim M. Hemsley,[2,6,7] Meghan L. Douglass,[2,7] Sarah J. Tamang,[2,7] Daniel Neumann,[2,7] Barbara M. King,[2,7] Helen Beard,[2,7] Paul J. Trim,[3] Leanne K. Winner,[2,7] Adeline A. Lau,[2,7] Marten F. Snel,[3] Cathy Gomila,[4] Jérôme Ausseil,[5] Xin Mei,[1] Laura Giersch,[1] Mark Plavsic,[1] and Ralph Laufer[1]

[1]Lysogene, 18–20 rue Jacques Dulud, 92200 Neuilly-sur-Seine, France; [2]Childhood Dementia Research Group, Hopwood Centre for Neurobiology, Lifelong Health Theme, South Australian Health and Medical Research Institute, Adelaide, SA 5000, Australia; [3]Mass Spectrometry Core Facility, SAHMRI, Adelaide, SA 5000, Australia; [4]Laboratoire de Biochimie Métabolique, CHU Amiens Picardie, 80054 Amiens, France; [5]Unité INSERM U1043, Centre de Physiopathologie Toulouse Purpan (CPTP), Université Paul Sabatier, 31024 Toulouse, France

Patients with mucopolysaccharidosis type IIIA (MPS IIIA) lack the lysosomal enzyme sulfamidase (SGSH), which is responsible for the degradation of heparan sulfate (HS). Build-up of undegraded HS results in severe progressive neurodegeneration for which there is currently no treatment. The ability of the vector adeno-associated virus (AAV)rh.10-CAG-SGSH (LYS-SAF302) to correct disease pathology was evaluated in a mouse model for MPS IIIA. LYS-SAF302 was administered to 5-week-old MPS IIIA mice at three different doses (8.6E+08, 4.1E+10, and 9.0E+10 vector genomes [vg]/animal) injected into the caudate putamen/striatum and thalamus. LYS-SAF302 was able to dose-dependently correct or significantly reduce HS storage, secondary accumulation of GM2 and GM3 gangliosides, ubiquitin-reactive axonal spheroid lesions, lysosomal expansion, and neuroinflammation at 12 weeks and 25 weeks post-dosing. To study SGSH distribution in the brain of large animals, LYS-SAF302 was injected into the subcortical white matter of dogs (1.0E+12 or 2.0E+12 vg/animal) and cynomolgus monkeys (7.2E+11 vg/animal). Increases of SGSH enzyme activity of at least 20% above endogenous levels were detected in 78% (dogs 4 weeks after injection) and 97% (monkeys 6 weeks after injection) of the total brain volume. Taken together, these data validate intraparenchymal AAV administration as a promising method to achieve widespread enzyme distribution and correction of disease pathology in MPS IIIA.

INTRODUCTION

Mucopolysaccharidosis type IIIA (MPS IIIA, OMIM #252900) is a lysosomal storage disorder caused by mutations in the *SGSH* gene that result in deficiency of the enzyme *N*-sulfoglucosamine sulfohydrolase (sulfamidase, EC 3.10.1.1) and subsequent accumulation of heparan sulfate (HS)-derived oligosaccharides.[1] Patients have relatively mild somatic symptoms; however, the central nervous system (CNS) is the primary site of pathology characterized by accumulation of HS and gangliosides, leading to neuroinflammation and severe neurodegeneration. As a result, patients experience a wide range of CNS-based symptoms, including delayed neurocognitive development, mental regression, rapid loss of social skills and learning ability, disturbed sleep, aggression, and hyperactivity, with death usually occurring during the second decade.[2] Therefore, the focus of new therapies is to treat the neurological manifestations associated with this disease.[3]

Gene therapy using adeno-associated virus (AAV) vectors with neuronal tropism holds promise for delivering SGSH to the brain, which is the organ most susceptible to toxicity caused by SGSH deficiency. Even though some AAV capsid serotypes or vectors with engineered capsid variants have been reported to cross the blood-brain barrier (BBB) in mice,[4,5] intravascular administration of AAV vectors in primates is much less efficient.[6–9] In nonhuman primates (NHPs), the most efficient route of delivery of an AAVrh.10 vector carrying the lysosomal enzyme arylsulfatase A was demonstrated to be direct injection into the subcortical white matter fiber tracts. This delivery route provided high enzyme expression and broad distribution throughout the primate brain, unlike administration by the intraventricular and intra-arterial routes, which failed to demonstrate measurable enzyme levels above controls.[10]

Direct intraparenchymal delivery of AAV vectors has been used in several clinical trials for neurological diseases, including lysosomal

Received 13 August 2019; accepted 2 December 2019;
https://doi.org/10.1016/j.omtm.2019.12.001.

[6]These authors contributed equally to this work.

[7]Present address: Childhood Dementia Research Group, College of Medicine and Public Health, Flinders University, Bedford Park, SA 5042, Australia.

Correspondence: Michaël Hocquemiller, Lysogene, 18–20 rue Jacques Dulud, 92200 Neuilly-sur-Seine, France.
E-mail: michael.hocquemiller@lysogene.com
Correspondence: Ralph Laufer, Lysogene, 18–20 rue Jacques Dulud, 92200 Neuilly-sur-Seine, France.
E-mail: ralph.laufer@lysogene.com

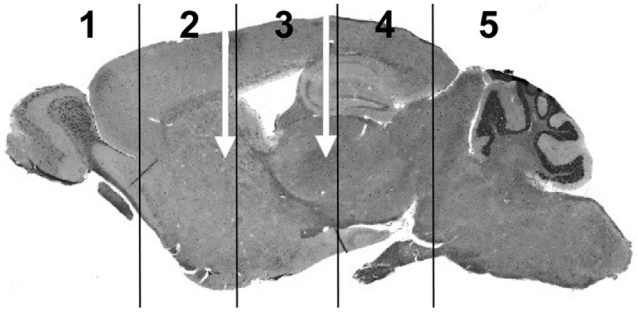

Figure 1. Intraparenchymal Injection of LYS-SAF302 in MPS IIIA Mice
The injection sites (white arrows) are shown from a lateral perspective and the locations of hemi-coronal brain slices 1–5 are indicated. MPS IIIA mice received stereotactic injection of LYS-SAF302 at 5 weeks of age using a Hamilton syringe (n = 10/sex/group). Vectors were administered at a dose of 8.6E+08 vg (low dose), 4.1E+10 vg (medium dose), or 9.0E+10 vg (high dose) in 8 μL delivered at 0.2 μL/min via 2 μL into each of the left and right striatum and 2 μL into each of the left and right thalamus.

disorders, as well as in preclinical disease models.[11,12] We previously obtained proof of concept for this approach in a MPS IIIA mouse model, where unilateral intracranial injection of an AAVrh.10 vector carrying SGSH and the sulfatase cofactor SUMF1, referred to as LYS-SAF301, resulted in ipsilateral restoration of SGSH and reduction in HS storage, the number of activated microglia, and, at later stages, reduced GM3 gangliosides and ubiquitin-positive lesions.[13] LYS-SAF301 was used in a phase 1/2 clinical trial for MPS IIIA,[14] in which four patients received 7.2E+11 vector genomes (vg) simultaneously via six injection sites at two depths in 60-μL deposits bilaterally to the white matter anterior, medial, and posterior to the basal ganglia. Safety data collected from inclusion, during the neurosurgery period and over the year of follow-up, showed good tolerance and absence of adverse events related to the injected product. Neuropsychological evaluations suggested a possible improvement in behavior, attention, and sleep in three out of four patients, with the youngest patient most likely to display a neurocognitive benefit.

We recently designed a second-generation, improved gene therapy vector, referred to as LYS-SAF302. LYS-SAF302 is an AAVrh.10 vector containing a stronger gene promoter (CAG versus murine phosphoglycerate kinase [mPGK] in LYS-SAF301), and it carries SGSH as a single transgene. In short-term (4-week) studies, LYS-SAF302 was shown to be about 3-fold more potent in directing brain expression of SGSH following intrastriatal administration in MPS IIIA mice.[15] The objective of the present work was to study the long-term effects of this vector on lysosomal pathology in MPS IIIA mice. In addition, we asked the question whether LYS-SAF302, administered by an improved delivery technique into white matter fiber tracts, was able to achieve therapeutically relevant SGSH expression and broad enzyme distribution in the brain of two large animal species, dogs and cynomolgus monkeys. The results of the present study supported the initiation of a pivotal phase 2/3 clinical study with LYS-SAF302 for the treatment of MPS IIIA.

RESULTS

Mouse Study

LYS-SAF302 was administered to 5- to 6-week-old MPS IIIA mice (n = 10/sex/group) at three different doses (8.6E+08, 4.1E+10, and 9.0E+10 vg/animal) injected into the caudate putamen/striatum and thalamus (Figure 1). A total of 150 animals were successfully treated with one of three doses of LYS-SAF302 (n = 90) or vehicle (n = 60). Of these, 100 mice (50 per time point) were used for the analyses described in this paper, except for survival and body weight measurements, which included all live animals. Animals were sacrificed (n = 5/sex/group) at 17 weeks of age (12 weeks post-injection) or 30 weeks of age (25 weeks post-injection) for brain tissue analysis.

As summarized in Table S1, there were 10 (out of 150 mice) unanticipated deaths post-surgery to the time at which the final cohort of mice was euthanized (30 weeks of age). Furthermore, three mice were observed to exhibit a decline in health or were observed to have a seizure, necessitating euthanasia during this period. One additional mouse (MPS IIIA vehicle-treated) required euthanasia due to an eye lesion that was unresponsive to antibiotic treatment. Thus, a total of 13 mice were found dead or had to be euthanized for unknown causes during the in-life period of the study. These mice were stratified across groups as follows: no unaffected vehicle-treated mice, one MPS IIIA vehicle-treated mouse, two MPS IIIA low dose-treated mice, five MPS IIIA medium dose-treated mice, and five MPS IIIA high dose-treated mice. There was no statistically significant difference between the numbers of deaths in the vehicle-treated (1/30) versus vector-treated (12/90) groups of MPS IIIA mice ($p = 0.13$ for the relationship, chi-square test). Post-mortem histological tissue analysis was performed on 8 out of the 13 animals; tissues from the other animals were not of sufficiently good condition for analysis. With the exception of a low dose-treated MPS IIIA mouse exhibiting meningoencephalitis post-mortem, the cause of the deaths or ill health requiring euthanasia could not be determined from post-mortem tissue analysis (see Table S1). The cause of meningoencephalitis is unknown but seems not to be related to LYS-SAF302, as only 1 mouse out of 90 injected with LYS-SAF302 had this adverse event.

Average body weights of MPS IIIA vehicle-treated mice rose faster than did those of unaffected vehicle-treated mice (Figure S1). While the weights of MPS IIIA vehicle-treated mice and of MPS IIIA low dose-treated mice maintained a similar trajectory, those of MPS IIIA medium dose-treated mice and MPS IIIA high dose-treated mice exhibited closer similarity to the body weights of unaffected vehicle-treated mice with time post-injection to 30 weeks of age, in both male and female cohorts.

At 12 weeks post-injection, there was an increase in liver and spleen weights with disease, and dose-dependent reductions were apparent in treated mice (Figure S2). By 25 weeks post-injection, in addition to liver and spleen, differences between the two vehicle-treated groups

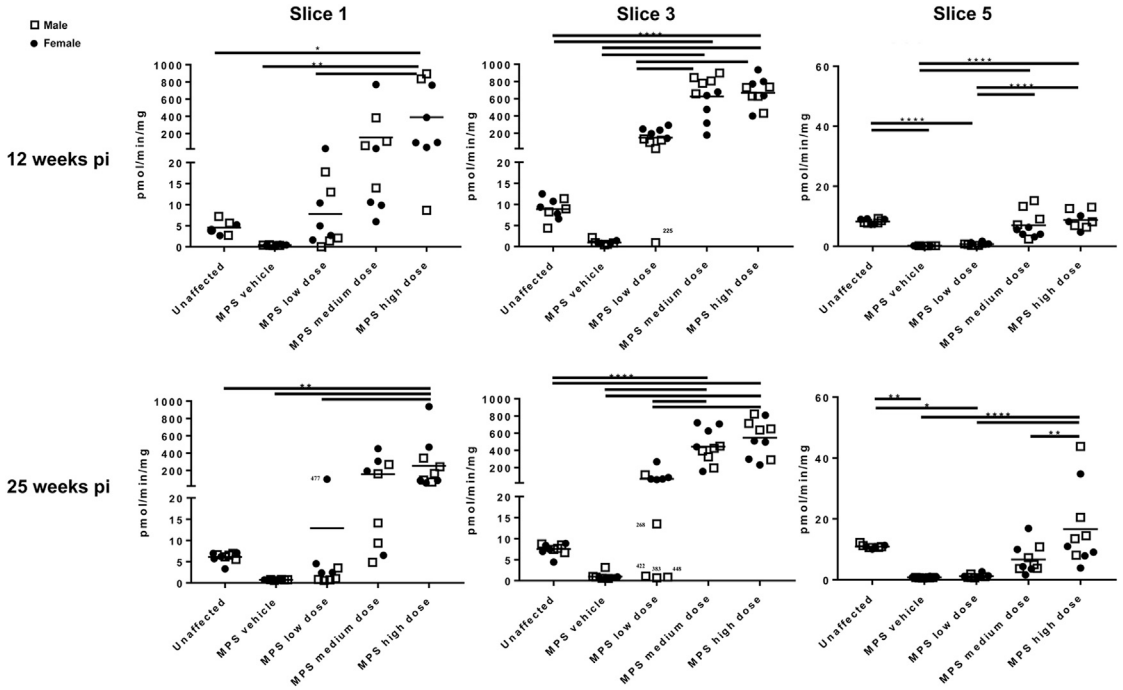

Figure 2. SGSH Activity in Brain Slices of MPS IIIA Mice at 12 and 25 Weeks Post-injection

SGSH activity was measured in individual brain slices 1, 3, and 5 according to the map given in Figure 1. Mouse #225 (17-week-old male in MPS IIIA low-dose group) was an outlier in each assay, exhibiting no increase in SGSH activity (compare with MPS IIIA vehicle mice). In the 30-week cohort, male low dose-treated MPS IIIA mice #422, #383, and #448 were outliers, exhibiting no increase in SGSH activity (compare with MPS IIIA vehicle mice). *p < 0.05, **p < 0.01, ****p < 0.0001 calculated from one-way ANOVA with Bonferroni's multiple comparisons test.

with regard to tissue weight were also seen in male but not female brain, heart, and kidney. Dose-dependent reductions in organ weight were seen in the heart and kidney of LYS-SAF302-treated males and in the brain of LYS-SAF302-treated mice of both sexes.

Dose-Dependent Increases in SGSH Enzyme Activity across All Brain Regions

Dose-dependent increases in SGSH enzyme activity were observed in all brain regions, with the largest amount of enzyme detectable in slice 3, which contains an injection site (Figure 2). The amount of active enzyme detected in each brain slice was maintained with time and was dependent on the dose of LYS-SAF302. Variability in enzyme activity was seen within treatment groups; this might be related to the amount of reflux from the injection syringe noted at the time of surgery (i.e., viral genomes actually delivered to the injection region), or variable diffusion of vector from the injection site, as potentially suggested by the fact that variability seemed to be higher as the distance from the injection site increased (see Figure 2).

Dose-Dependent Decreases in Primary HS Accumulation across All Brain Regions

The same brain slices examined for SGSH activity were evaluated for total HS content (Figure 3). As anticipated, regardless of age, all vehicle-treated MPS IIIA mice exhibited significant increases in HS in all three brain slices versus those of unaffected vehicle-treated mice. There appeared to be no impact of sex on HS level in the vehicle-treated cohorts or the LYS-SAF302-treated cohorts. Brain slices 1 and 3 exhibited the greatest reduction in HS content following treatment. Normal HS levels were attained at all three doses of LYS-SAF302 in slice 3 and at the two higher doses in slice 1. The treatment effect was also strong in slice 5, particularly at the higher two doses. The effect of treatment was maintained to 25 weeks post-injection (see Figure 3).

Dose-Dependent Decreases in Neuropathological Biomarkers

Secondary accumulation of gangliosides has been reported in several of the MPS diseases, including MPS IIIA.[16] GM2 and GM3 was measured in brain slices 1, 3, and 5 at 12 weeks and 25 weeks after treatment (data of slice 3 at 25 weeks post-injection are presented in Figures 4A and 4B; slice 1 and 5 data at 25 weeks post-injection are presented in Figure S3). All vehicle-treated MPS IIIA mice exhibited significant increases in GM2 and GM3 in all three brain slices, an outcome observable at each of the two euthanasia ages. There appeared to be no impact of sex on ganglioside levels in any of the vehicle-treated or LYS-SAF302-treated cohorts. Each of the three doses of LYS-SAF302 resulted in normalization of GM2 and GM3 ganglioside levels in brain slice 1 and 3 (Figures 4A and 4B; Figure S3). While ganglioside levels were not normalized in slice 5, there was a reduction in GM2 and GM3 levels post-treatment, which was particularly notable at the higher doses (Figure S3).

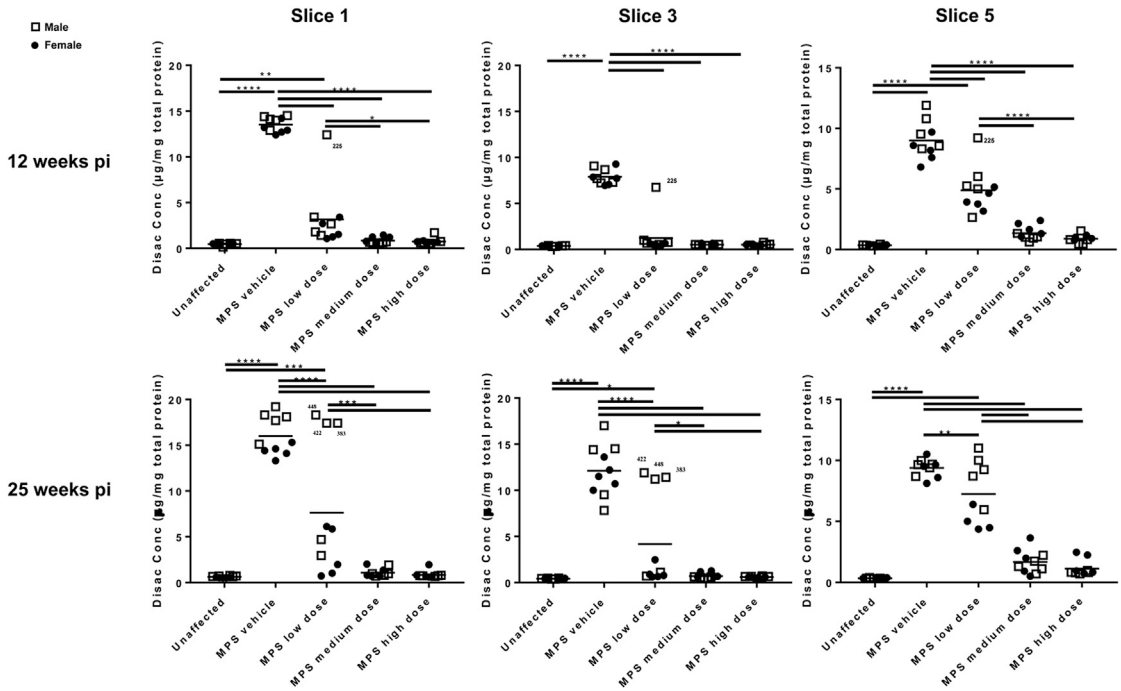

Figure 3. Total Amount of HS in Brain Slices of MPS IIIA Mice at 12 and 25 Weeks Post-injection

HS was quantified in individual brain slices 1, 3, and 5 according to the map given in Figure 1. Mouse #225 (17-week-old male in MPS IIIA low-dose group) was an outlier in each assay, exhibiting no reduction in HS (compare with MPS IIIA vehicle mice). In the 30-week cohort, male low dose-treated MPS IIIA mice #422, #383, and #448 were outliers, exhibiting no reduction in HS (compare with MPS IIIA vehicle mice). This is in keeping with the low amount of SGSH activity recorded for these mouse samples (Figure 2). *$p < 0.05$, **$p < 0.01$, ***$p < 0.001$, ****$p < 0.0001$ calculated from one-way ANOVA with Bonferroni's multiple comparisons test.

Characteristic neuronal morphological abnormalities associated with MPS IIIA, consisting of endosomal and lysosomal expansion and spheroidal lesions,[17] were evaluated in several brain areas at 12 and 25 weeks after treatment. Figure 4C depicts 25-week results from inferior colliculus or dentate gyrus, as examples representative of other brain regions, while additional time points and brain regions are shown in Figure S4. No particular brain region is known to be more relevant to the disease than another. Endosomal and lysosomal expansion reflected by lysosomal integral membrane protein-2 (LIMP-2) immunohistochemistry was significantly increased in the vast majority of the MPS IIIA vehicle-treated mouse brain areas examined, in both the 12 and 25 weeks post-injection cull groups. Dose-dependent reductions in LIMP-2 staining were observed across the rostro-caudal axis of the brain and were maintained to 25 weeks post-treatment, particularly in mice treated with the medium and high doses of LYS-SAF302 (Figure 4C; Figure S4; data not shown). The number of ubiquitin-positive spheroidal lesions >5 µm was evaluated and at both cull times, and all regions exhibited a significant increase in ubiquitin-reactive lesions in vehicle-treated MPS IIIA mouse brain compared to age-matched unaffected vehicle-treated mice. All LYS-SAF302 doses significantly reduced the number of lesions in all brain areas examined, except the corpus callosum (Figure 4D; Figure S5; data not shown).

Neuroinflammation associated with MPS IIIA[18,19] was evaluated by the presence of astroglial activation using immunohistochemical detection of glial fibrillary acidic protein (GFAP) and by the presence of activated microglia using histochemical staining of isolectin B4-reactive amoeboid microglia. With the exception of the dentate gyrus and cerebellum, significantly increased GFAP expression indicative of astrocyte activation was observed in vehicle-treated MPS IIIA mouse brain regions at both time points compared to that of age-matched unaffected vehicle-treated mice (Figure 4E; Figure S6; data not shown). A treatment effect was difficult to discern at 12 weeks post-injection, with no reduction in GFAP expression noted in the caudate and thalamus (data not shown) and the inferior colliculus (Figure 4E). There was a reduction in GFAP staining in the brainstem and rostral cortex at the early cull time point (Figure S6). By 25 weeks post-injection, the inferior colliculus exhibited significant reductions in GFAP at the higher two doses (Figure 4E). However, at this time point, significantly more GFAP was observed in medium and high dose-treated MPS IIIA mouse rostral cortex (midline) and caudate injection level compared to low dose-treated MPS IIIA mice (data not shown). It remains to be determined whether this may reflect cellular toxicity due to locally high SGSH expression.

Large numbers of activated microglia were apparent in vehicle-treated MPS IIIA mouse brain compared to vehicle-treated unaffected mouse brain (Figure 4F; Figure S7). All three doses of LYS-SAF302 essentially resulted in normalization of microglial morphology, interpreted as deactivation, across the more rostral/central aspects of brain. This outcome was maintained to 25 weeks post-injection.

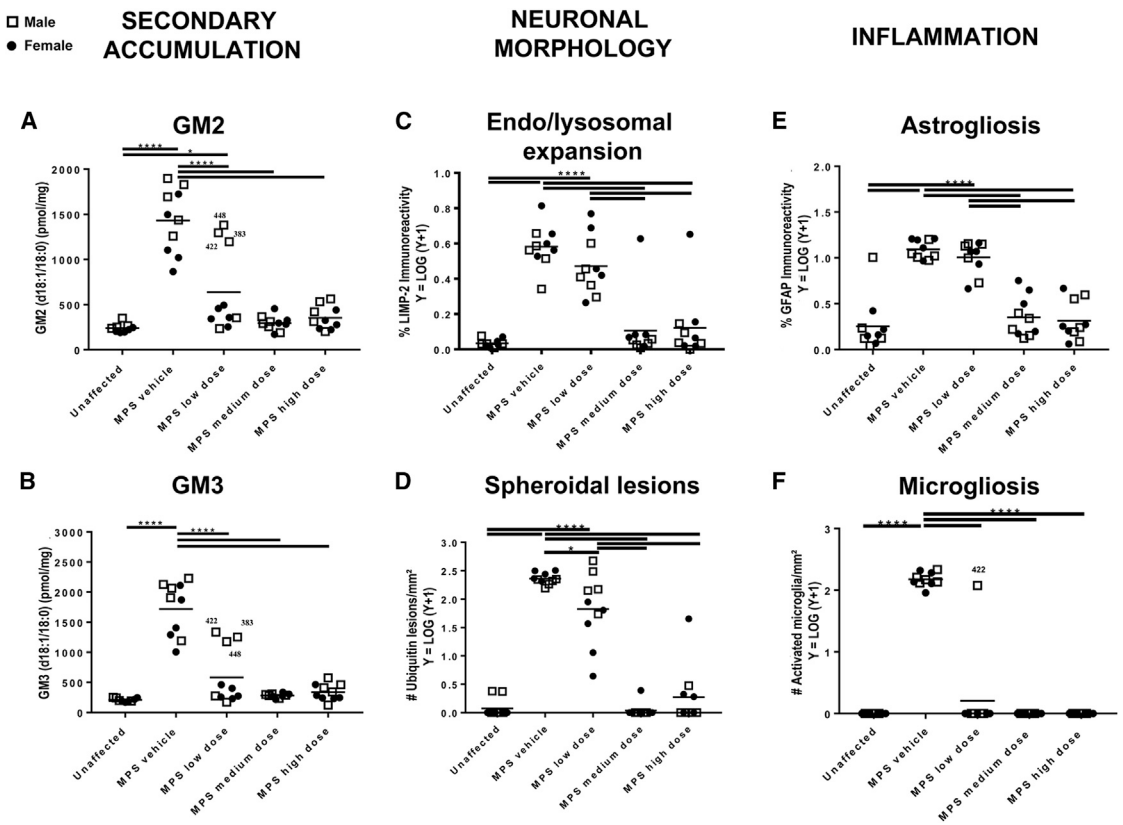

Figure 4. Disease-Associated Lesions in the Brain of MPS IIIA Mice at 25 Weeks Post-injection

Disease lesions associated with MPS IIIA were analyzed at 25 weeks post-treatment. (A and B) Quantification of the secondary accumulation of GM2 (A) and GM3 (B) ganglioside in brain slice 3. Male low dose-treated MPS IIIA mice #422, #383, and #448 were outliers, exhibiting no reduction in gangliosides (compare with MPS IIIA vehicle mice). This is in keeping with the low amount of SGSH activity and the high amount of HS recorded for these mouse samples (Figures 2 and 3) (C) Endosomal/lysosomal system expansion assessed by LIMP-2 staining in inferior colliculus. (D) Number of axonal spheroids, assessed by ubiquitin staining in inferior colliculus. (E) Extent of astrogliosis, assessed by GFAP staining in inferior colliculus. (F) Number of reactive amoeboid-shaped microglia, assessed by isolectin B4 staining, in dentate gyrus. *$p < 0.05$, ****$p < 0.0001$ calculated from one-way ANOVA with Bonferroni's multiple comparisons test.

The results for dentate gyrus at 25 weeks post-injection are presented in Figure 4F as an example representative of additional brain regions (data not shown). Dose-dependent outcomes were noted in brainstem (Figure S7) and cerebellum (data not shown), with the low dose failing to deactivate microglia in the latter, at either time point.

Evaluation of Blood Sera for Anti-AAVrh.10 and Anti-hSGSH Antibodies

In the 12-week post-injection cohort, all medium and high dose-treated mouse sera exhibited anti-AAVrh.10 antibodies (Figure S8). Sera from 4 (of 10) low dose-treated mice exhibited anti-AAVrh.10 antibodies. In the 30-week cull cohort, anti-AAVrh.10 antibodies were detected in one low dose-treated and all medium dose- and high dose-treated animals.

Anti-hSGSH antibody titers were also measured (Figure S8). Only one 12-week post-injection mouse exhibited an antibody titer that is considered to be significant (male MPS IIIA mouse treated with a high dose). In the 25-week post-injection cohort, three low dose-, two medium dose-, and three high dose-treated mice had anti-SGSH antibody titers that were deemed to be significant.

Taken together, these data show that despite the presence of a humoral immune response in some animals to AAVrh.10 and the hSGSH protein, LYS SAF302 is capable of mediating sustained dose-dependent effects on MPS IIIA-related brain pathology over the time frame of this experiment, i.e., up to 25 weeks post-injection. The greatest effect of treatment was proximal to the injection regions, particularly with the low dose of LYS-SAF302. Due to anatomical differences between mouse and human brain, the injection sites used in the mouse study are not those selected for use in patients with MPS IIIA. Injection of LYS-SAF302 into subcortical white matter, which is the route of administration intended for human clinical studies, was next assessed in dogs and NHPs.

Dog Study

LYS-SAF302 was administered to healthy male beagle dogs together with the MRI contrast agent gadolinium by infusion into the

Table 1. Biodistribution Data in Dog Brain 4 Weeks Post-injection

Animal	#106		#108		#109	
Hemisphere:	Right	Left	Right	Left	Right	Left
Vector concentration (vg/mL)	1.0E+12	1.0E+12	1.0E+12	1.0E+12	1.0E+12	1.0E+12
No. of deposits per hemisphere	1	1	1	1	2	2
Volume per deposit (μL)	500	500	500	500	500	500
Speed of injection (μL/min)	10	10	10	10	10	10
Total dose per hemisphere (vg)	5.0E+11	5.0E+11	5.0E+11	5.0E+11	1.0E+12	1.0E+12
Total volume injected (vi) per hemisphere (cm^3)	0.50	0.50	0.50	0.50	1.00	1.00
Volume of distribution (vd) of gadolinium (cm^3)	1.56	1.43	1.50	1.39	3.63	2.92
vd gadolinium/vi	3.1	2.9	3.0	2.8	3.6	2.9
No. of punches for qPCR analysis	40	40	40	40	33	33
No. of punches >0.1 cp/cell	14	15	13	17	10	14
% of punches >0.1 cp/cell	35%	38%	33%	43%	30%	42%
No. of punches for enzyme analysis	40	40	40	40	33	33
No. of punches >20% enzyme increase	29	33	30	27	30	26
% of punches >20% enzyme increase	73%	83%	75%	68%	91%	79%

Data from six hemispheres injected with LYS-SAF302 from three dogs with 4 weeks post-injection endpoint. cp, copies.

white matter using convection-enhanced delivery at a flow rate of 10 μL/min. The study goal was to investigate vector distribution and performance of the SmartFlow cannula device used for drug administration. Two infusions (one per hemisphere) of 500 μL of non-diluted drug product at a concentration of 1.0E+12 vg/mL were administered to two animals (#106 and #108), resulting in a total dose of 1.0E+12 vg, and four infusions (two per hemisphere) were administered in one animal (#109), resulting in a total dose of 2.0E+12 vg (Table 1). As 500 μL is the maximal volume that could be administered at each site using this technique, these doses represent maximal feasible doses per injection, and they were chosen to maximize the chance of obtaining robust vector transduction and distribution.

MRI was performed immediately after surgery, and collected images were analyzed using OsiriX software to quantify the gadolinium signal (Figure 5). The volumes of gadolinium signal per hemisphere were then normalized to the corresponding injection volumes and expressed as the ratio of gadolinium distribution volume/injected volume. Results indicate that the SmartFlow cannula performed well with no reflux detected. The administration of 500 μL per tract of LYS-SAF302 was found to be associated with leakage into the lateral ventricle in both the rostral and caudal injection tracts. This is likely due to due to the very narrow white fiber tracts of approximately 75 cm^3 in dog brain (Figures 5B and 5C). The mean ratio of gadolinium distribution volume/injected volume was 3.1 ± 0.2 (Table 1).

Vector copy analysis was performed by TaqMan qPCR with primers and probe specific for the transgene. A threshold of 0.1 vector copy per cell was set up based on the observation that this (or higher) level was always associated with an SGSH activity increase in dog brain samples. At 4 weeks after injection of LYS-SAF302, more than 0.1 vector copy per cell was found in 37% ± 4% of the brain punches tested (Table 1; Figure S9).

SGSH enzyme activity analysis was also performed on brain punches, and results were expressed as the percentage of endogenous activity. Four weeks after injection of LYS-SAF302, greater than 20% SGSH activity increase was found in 78% ± 6% of the brain punches tested (Table 1; Figure S9). A possible explanation for the lack of increase in vector DNA or SGSH activity between dogs that received one or two injections is that because of the high volume injected, significant leakage into the lateral ventricles occurred.

NHP Study

LYS-SAF302 was administered to healthy male cynomolgus monkeys into the subcortical white matter using convection-enhanced delivery at a flow rate of 5 μL/min. The goal of the study was to investigate SGSH activity distribution in NHP brain following LYS-SAF302 administration at a dose equivalent to the intended human clinical dose of 7E+12 vg/kg brain weight. The latter was chosen based on the dose used in phase 1, the safety margin from an independently performed GLP toxicology study, and the maximal dose that can be used in humans due to manufacturing and anatomical considerations.

To avoid leakage into the ventricles, a lower injection volume (50 μL) was used than in the dog study. This volume was also chosen because it represents a brain-weight-normalized volume (0.7 μL/g) that would be compatible to injection into a human patient's brain, i.e., injection of about 700 μL in a child's brain of about 1,000 g, which is technically feasible. Four infusions (two per hemisphere) of 50 μL of non-diluted drug product LYS-SAF302 at a concentration of 3.6E+12 vg/mL were

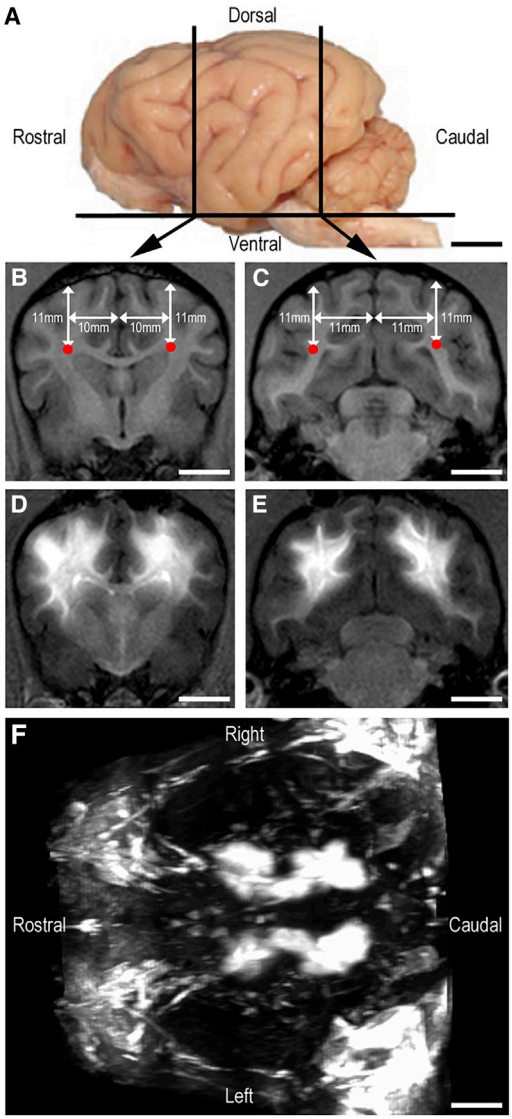

Figure 5. Gadolinium Diffusion in Dog Brain

Representation of dog #109 that received four injections of 500 μL (two per hemisphere) of LYS-SAF302 with the MRI contrast agent gadolinium (5 mmol) into the white matter at 10 μL/min (total dose, 2.0E+12 vg). (A) Left lateral view of a dog brain with the position of coronal sections that include sites of injection. (B and C) MRI images of coronal rostral (B) and caudal (C) sections before injection with planned site of injection represented with red dot spots. (D and E) MRI images of coronal rostral (D) and caudal (E) sections after injection with gadolinium signal visible into the white matter. (F) Anterior view of 3D reconstruction of MRI images with gadolinium signal visible in both hemispheres along the rostro-caudal axis of the white matter. Scale bars, 10 mm.

performed in two animals (#169I and #763E), resulting in a total dose of 7.2E+11 vg (Table 2).

Prior to injection, two animals were found seronegative for AAVrh.10 neutralizing factors and one was found weakly positive (titer 1:10). Six weeks after injection, the animal injected with vehicle was still seronegative and AAVrh.10 neutralizing factors were detected at a titer of 1:1,000 in both animals injected with LYS-SAF302. No anti-hSGSH antibodies were detected before and 6 weeks after injection in any of the three animals (data not shown).

Vector copy analysis was performed using TaqMan qPCR with primers and probe specific for the transgene. A threshold of 0.1 vector copy per cell was set as in the dog study. Six weeks after administration of LYS-SAF302, more than 0.1 vector copy per cell was found in 11% ± 1% of the brain punches tested (Table 2; Figure S10).

SGSH enzyme activity analysis was also performed, and results were expressed as the percentage of endogenous activity. Six weeks after injection, a greater than 20% SGSH activity increase was found in 97% ± 2% of the brain punches tested (Table 2; Figure 6; Figure S10).

When normalized to the volume injected, vector diffusion was broader in the NHP study (11% of the brain covered with 100 μL injected) compared to the dog study (37% covered with 500 μL or 1 mL injected), reflecting reduced leakage of injected volumes into the lateral ventricles due to larger white fiber tracts of the NHP brain and lower injected volume. Despite lower absolute levels of vector diffusion in NHP compared to dog, SGSH activity was more broadly distributed throughout the NHP brain (at least 20% activity increase in 97% of the brain versus 78% in dogs). The differences observed between the two studies could be due to possible species differences or may reflect better enzyme secretion and broad diffusion in the NHP brain after a 6-week period compared to a 4-week period in dogs.

DISCUSSION

MPS IIIA, a lysosomal storage disease with predominantly neurological pathology, is an ideal candidate for gene therapy using AAV vectors delivered directly into the CNS. AAVrh.10 is a neuronotropic AAV serotype discovered from latent genomes in primate tissue.[20] Quantitative measures of transduction identified both AAV9 and AAVrh.10 as significantly more efficient than either AAV1 or AAV5 at transducing cerebral cortex, caudate nucleus, thalamus, and internal capsule after brain injection. Fluorescence co-labeling with cell-type-specific antibodies demonstrated that both AAV9 and AAVrh.10 primarily transduce neurons, although glial transduction was also identified.[15,21] AAVrh.10 vectors have been used in clinical trials for MPS IIIA[22], neuronal ceroid lipofuscinosis,[23] and metachromatic leukodystrophy,[24] and they are being explored for several other neurological indications.[11]

A first-generation recombinant AAAVrh.10 vector, LYS-SAF301, which contains the human SGSH and SUMF1 genes under the control of the mPGK promoter, was previously administered by intracerebral injection to four children with MPS IIIA in a phase 1/2 trial. Vector administration was safe and behavioral improvements were observed in three out of four patients, with a suggested cognitive benefit in the youngest patient, which was more limited as patient age and presumed disease burden increased.[22] We recently designed

Table 2. Biodistribution Data in NHP Brain at 6 Weeks Post-injection

Animal	#169I		#763E	
Hemisphere:	Right	Left	Right	Left
Vector concentration (vg/mL)	3.6E+12	3.6E+12	3.6E+12	3.6E+12
No. of deposits per hemisphere	2	2	2	2
Volume per deposit (μL)	50	50	50	50
Speed of injection (μL/min)	5	5	5	5
Total dose per hemisphere (vg)	3.6E+11	3.6E+11	3.6E+11	3.6E+11
No. of punches for qPCR analysis	46	48	48	43
No. of punches >0.1 cp/cell	6	5	4	5
No. of punches >0.1 cp/cell	13%	10%	8%	12%
No. of punches for enzyme analysis	51	53	52	50
No. of punches >20% enzyme increase	50	53	50	46
% of punches >20% enzyme increase	98%	100%	96%	92%

Data from four hemispheres injected with LYS-SAF302 from two NHPs with 6 weeks post-injection endpoint. cp, copies.

an improved, second-generation vector, LYS-SAF302, which expresses a single gene, human SGSH, under the control of the CAG promoter. LYS-SAF302 was shown to be about 3-fold more potent than LYS-SAF301 in directing the expression of SGSH in the brain of MPS IIIA mice. In parallel, LYS-SAF302 was more efficacious in correcting lysosomal storage defects and inflammatory pathology at 4 weeks following intrastriatal dosing at 4E+09 vg/animal in this mouse model.[15] The results of the present study confirm and extend these observations, by demonstrating dose-dependent and long-term effects of LYS-SAF302 in MPS IIIA mice. While the production of anti-AAVrh.10 and anti-hSGSH antibodies did not appear to diminish the effectiveness of the therapy or cause any health issues for the mice, there were 13 unanticipated deaths of mice that required euthanasia in this study for which the cause has not been determined despite post-mortem tissue analysis. There is no statistically significant difference between the numbers of deaths in the vehicle group versus all LYS-SAF302 groups combined, but a role of the vector in these events, possibly because of locally high vector concentrations near the site of injection into gray matter brain nuclei, cannot currently be excluded.

In our previous efficacy study with LYS-SAF301, vector was administered unilaterally at a total dose of 7.5E+09 vg into the mouse striatum.[13] To provide broader and more uniform distribution of LYS-SAF302 and its transgene product in the brains of treated mice, the vector was injected bilaterally into both striatum and thalamus in the present study, using three different doses ranging from 8.6E+08 to 9.0E+10 vg. This procedure resulted in efficient, long-lasting, and dose-dependent increases in enzyme activity in all brain regions, with highest levels near the injection sites. Elevations in SGSH activity were accompanied by correction of biochemical abnormalities in the brain of MPS IIIA mice, in agreement with what has been previously reported using different vectors or delivery routes.[13,25–27] LYS-SAF302 was able to normalize HS and ganglioside accumulations and reduce pre-existing disease lesions, such as lysosomal expansion and microgliosis, which would have been present at significant levels at the time of dosing.[28] In addition, LYS-SAF302 was also able to prevent the onset of axonal spheroid lesions, as this type of lesion is slower to develop[28] and would have been present at lower levels or only in some brain regions at the time of treatment onset.

The ability of LYS-SAF302 to significantly reduce microgliosis in the brain of MPS IIIA mice is of particular relevance, as neuroinflammation mediated by activated microglia is thought to play a key role in MPS pathogenesis and disease progression.[18] Consistent with the present findings, 4-week treatment with LYS-SAF302 reduced inflammatory chemokines and cytokines in the brain of MPS IIIA mice.[15] The ability of LYS-SAF302 to cause a long-lasting reversal of the neuroinflammatory phenotype of microglia, which is thought to lead to and exacerbate neuronal damage in MPS IIIA,[18] could have profound implications for its therapeutic potential.

In the present study, even the lowest dose of LYS-SAF302 tested led to levels of SGSH activity in brain regions close to the injection site that were, on average, higher than those of wild-type mice. In those brain regions, a strong, nearly total correction of biochemical lysosomal storage defects was achieved. This result is consistent with previous reports showing that SGSH activity levels of 10%–20% of wild-type levels in the brain are sufficient to correct biochemical, cellular, and behavioral disease manifestations in MPS IIIA mice. These data were obtained by delivering SGSH to the brain of MPS IIIA mice using different modalities, including infusion of recombinant enzyme into the cerebrospinal fluid (CSF),[29] gene therapy with AAV vectors administered by intravascular or intra-CSF routes,[26,27] or bone marrow replacement with hematopoietic stem cells transduced *ex vivo* with an SGSH-expressing lentivirus.[30] The concept that such relatively low levels of SGSH are sufficient to correct disease manifestations is in line with the fact that the diagnosis of MPS IIIA is made on the basis of SGSH activity in fibroblasts or leukocytes that is less than 10% of average normal activity, and that non-affected carriers as well as normal individuals display a wide range of SGSH activity, with a lower limit that is about 20% of average normal levels.[31,32]

Even though several different treatment modalities, as described above, were successful in delivering SGSH to the brain of MPS IIIA mice, it is much more challenging to achieve efficient delivery of proteins into the brain of larger animals. Even though some AAV vector serotypes, such as AAV9, have been reported to cross the BBB in rodents, systemic administration is much less efficient in large animals, in particular NHPs.[6–9] The intravascular route of delivery in primates is limited by the extremely large doses required to achieve transduction in the brain and the resulting high off-target transduction of peripheral organs[6,9,33,34] and risk of systemic toxicity.[35] Likewise, intra-CSF administration required about 10-fold higher doses than did direct intraparenchymal delivery of AAV vectors, which clearly appears to be the most efficient route of administration to achieve strong and widespread transgene expression throughout the brain of NHPs.[10,24,33,36,37]

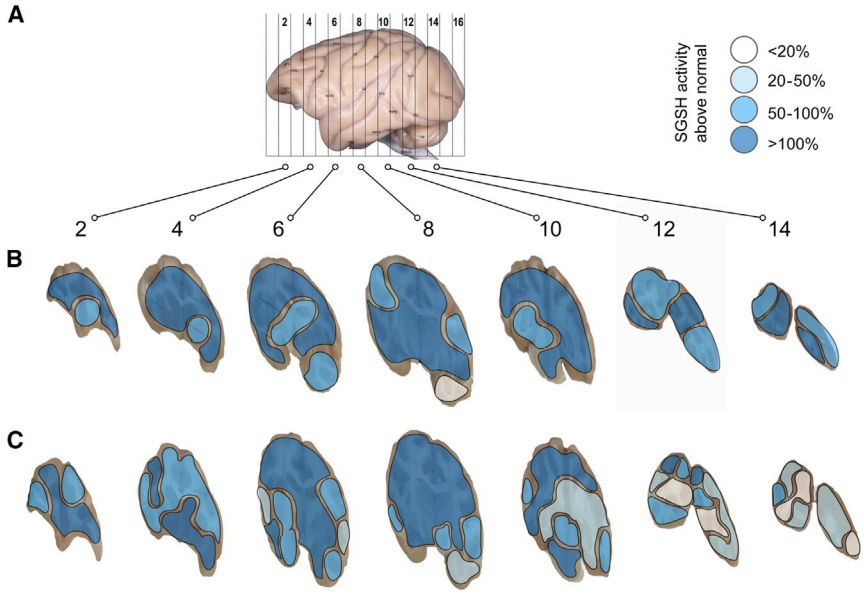

Figure 6. SGSH Activity Distribution in NHP Brain

Representation of SGSH activity in the brain of two NHPs that received four injections of 50 μL (two per hemisphere) of LYS-SAF302 into the white matter at 5 μL/min (total dose, 7.2E+11 vg). (A) Left lateral view of a NHP brain with the location of the hemi-coronal brain slices shown. Rostral injections were between slices 4 and 6 and caudal injections were between slices 8 and 10. (B and C) A greater than 20% increase of SGSH activity relative to vehicle-injected control was observed 6 weeks after injection in 99% of the brain punches analyzed for NHP #169I (B) and 94% of the brain punches analyzed for NHP #763E (C). Numerical data are presented in Figure S10.

To assess whether the therapeutic target of 10%–20% of normal enzyme activity can be achieved by delivering LYS-SAF302 into the brain of large animals, the vector (~1E+13 vg/g brain) was injected into subcortical white matter tracts of dogs and cynomolgus monkeys, followed by quantification of vector DNA and SGSH enzyme activity in brain sections. Injection into white matter fiber tracts leads to more uniform brain distribution than injection into gray matter nuclei [10], and avoids high local exposure to vector and transgene product in neuronal cell body-rich regions. Convection-enhanced delivery has been shown to enhance delivery and brain distribution of infusates into the CNS.[38–40] A reflux-resistant cannula that allows for higher flow rates and infusion volumes than the simple cannulae used in previous clinical studies[22] was employed to infuse LYS-SAF302. In the dog study, co-infusion of gadolinium allowed us to assess the degree of penetration of the dosing solution into the brain, showing that despite some leakage into the lateral ventricles, there was extensive distribution into both rostral and caudal brain regions. While significant amounts of vector DNA were found in only 37% of brain punches, increases of SGSH activity of 20% or greater relative to vehicle-treated animals were found in 78% of the brain punches tested 4 weeks after injection. Similarly, a comparable dose of LYS-SAF302 injected into white matter fiber tracts in cynomolgus monkeys led to the presence of vector DNA in a limited proportion (11%) of brain punches, but a wide distribution of SGSH enzymatic activity of 20% or more of control levels in the near totality (97%) of the NHP brain 6 weeks after injection.

Several factors can contribute to widespread brain expression of SGSH, including diffusion/convection of the vector infusate, axonal and trans-synaptic transport of the AAV vector,[41,42] and axonal and trans-synaptic transport of SGSH. The finding that in both dog and monkey brain SGSH enzyme activity was more widespread than that of the encoding vector DNA suggests that the enzyme protein is transported along axonal connection pathways and reaches brain areas distant from the site of vector transduction, as previously observed with other AAV-based gene therapy in lysosomal storage disease.[43,44] Lysosomal enzymes undergo transport from cell bodies of transduced neurons along the axonal cytoplasm into neuronal projection areas, followed by secretion from axon terminals into the extracellular space.[42,45–48] Lysosomal enzymes can be secreted, taken up by neighboring cells via mannose-6-phosphate receptor-mediated endocytosis, and subsequently enter lysosomes, where they can functionally replace mutant lysosomal enzymes and correct storage defects, a phenomenon known as cross-correction.[49,50] In particular, human SGSH was shown to be able to correct the storage phenotype of MPS IIIA fibroblasts after endocytosis via the mannose-6-phosphate receptor.[51] The difference between vector copy number and enzyme distribution was more pronounced in NHPs than in dogs, potentially due to differences in study length and the possibility that vector distribution in dogs was boosted by a higher injection volume.

In conclusion, the results of the present study validate LYS-SAF302 as a promising new candidate for gene therapy of MPS IIIA. In the phase 1/2 trial conducted with the first-generation vector LYS-SAF301 in four children with MPS IIIA at a dose of 7.2E+08 vg/g brain, encouraging signs of improvement were noted. Using the second-generation vector, which is about 3-fold more potent, at a 10-fold higher clinical dose (7.2E+09 vg/g brain) and using an optimized delivery technique, significantly higher efficacy might be expected. Extrapolating the results of the dog and monkey studies to the human brain on the basis of brain volume (weight), it appears that this relatively low dose of LYS-SAF302 should be able to restore at least 20% of normal SGSH activity throughout the brain of an MPS IIIA patient. As discussed above, this level of restoration of enzyme activity is predicted to have a significant positive impact on disease progression.

MATERIALS AND METHODS

Mice

The congenic C57BL/6 MPS IIIA mouse strain was created after 10 backcrosses to inbred C57BL/6 mice.[52] The mouse study was

conducted at the Women's and Children's Health Network (WCHN) Animal Care Facility (Adelaide, SA, Australia) with the approval of the WCHN Animal Ethics Committee, in accordance with the guidelines of the National Health and Medical Research Council of Australia on the use and care of experimental animals.

Dogs

Healthy, male beagle dogs (weighing 7.50–9.90 kg prior to surgery) were received from Marshall BioResources (North Rose, NY, USA). The dog study was conducted at MPI Research (Mattawan, MI, USA) in accordance with standard operating procedures and based on the current International Council for Harmonisation Harmonised Tripartite Guidelines and generally accepted procedures for the testing of pharmaceutical compounds and in accordance with the US Department of Agriculture's (USDA) Animal Welfare Act (9 CFR, parts 1, 2, and 3) and the *Guide for the Care and Use of Laboratory Animals* (Institute of Laboratory Animal Resources, National Academies Press, Washington, DC, 2011).

NHPs

Healthy, male cynomolgus monkeys (*Macaca fascicularis*) (4.2–4.5 years old prior to surgery) were received from Noveprim (Mauritius Island). The NHP study was conducted at MIRCen (Fontenay-aux-Roses, France) according to European regulations (EU Directive 2010/63) and in compliance with Standards for Humane Care and Use of Laboratory Animals of the Office of Laboratory Animal Welfare (OLAW #A5826-01) in a facility authorized by local authorities (authorization #B92-032-02).

AAV Production and Titration

LYS-SAF302 is an AAV.rh10 vector that carries a defective AAV2 genome containing the human *SGSH* gene driven by cytomegalovirus enhancer fused to a chicken β-actin promoter/rabbit β-globin intron (CAG promoter).[13] LYS-SAF302 vector batches were supplied by Novasep (Gosselies, Belgium). Briefly, vectors were manufactured via triple transient transfection of adherent human embryonic kidney (HEK293) cells. After the cell harvest and lysis steps, the crude viral lysate of rAAV underwent several purification steps, including clarification by depth filtration, affinity chromatography using AVB resin, and tangential flow filtration. The formulation buffer (phosphate-buffered saline [PBS]) was used to dilute LYS-SAF302 to the target vector concentration and then sterilized by 0.2-μm filtration.

LYS-SAF302 titers were measured using a validated TaqMan qPCR method using a forward primer (5′-CCA GCC CCT CCA CAA TGA-3′), a reverse primer (5′-CAC TGG AGT GGC AAC TTC CA-3′), and a probe (5′-CAT CCC TGT GAC CCC-3′).

Intracranial Injections

Mice received intraparenchymal injections at 5–6 weeks of age of either vehicle (PBS) or one of three different doses of LYS-SAF302 (total doses of 8.6E+8, 4.1E+10, or 9.0E+10 vg). Induction and maintenance of surgical depth anesthesia was at 1%–5% isoflurane in a flow of 1–2 L/min oxygen. Once mice were unresponsive, they were secured in a stereotaxic frame (David Kopf Instruments, Tujunga, CA, USA), the scalp was resected, and a burr hole was made using a hand drill fitted with a 0.5-mm drill bit (Flintware, Adelaide, SA, Australia). Mice received a total of 8 μL of LYS-SAF302 or vehicle (2 μL per site) at a rate of 0.2 μL/min via 27G needles connected via polyethylene tubing to Hamilton syringes. Bilateral target sites (with respect to bregma) were as follows: posterior aspect of the striatum attempting to include white fiber tracts, 0.75 mm anterior, 1.5 mm lateral, 3 mm ventral; and the thalamus, 2 mm posterior, 1.5 mm lateral, 3 mm ventral. Injection co-ordinates are based on the mouse brain atlas by Paxinos and Franklin.[53] Mice received 0.05 mg/kg buprenorphine for pain relief and 4% dextrose in saline for fluid replacement during the procedure.

Dogs received intraparenchymal injections of either PBS (n = 2) or LYS-SAF302 (n = 3) together with the MRI contrast agent gadolinium (5 mmol). The animals were immunosuppressed beginning on day −1 through euthanasia to avoid immune reaction against the transgene. Immunosuppressants used were a combination of mycophenolate mofetil (MFF) (10–50 mg/kg twice daily via oral gavage) and tacrolimus (1 mg/kg/day via capsule dose, 0.16 mg/kg/day intramuscular injection). After anesthesia, animals were placed in ventral recumbency. A midline dorsal incision was made on the dorsal surface of the skull extending to cervical region. The base of the skull was exposed and an MRI fiducial was placed. The skin incision was temporarily closed with sutures and animals were transported to the MRI unit for coronal and sagittal imaging of the brain. Once the MRI scans were collected, they were uploaded to OsiriX MD for targeting purposes. The target was approximately 15 mm caudal of the coronal suture and 10 mm left and right lateral of the midline. The animal was placed in a head immobilizer frame and the incision was reopened. A bilateral craniotomy was performed with a burr. Based on the stereotaxic coordinates from OsiriX, the SmartFlow cannulas (MRI Interventions, Irvine, CA, USA) were inserted into the target area. Two or four infusions of 500 μL were administered in each animal (one or two per hemisphere) into the white matter at a flow rate of 10 μL/min (total dose of 1.0E+12 or 2.0E+12 vg).

NHPs received intraparenchymal injections of either PBS (n = 1) or LYS-SAF302 (n = 2). Animals were anesthetized with ketamine/xylazine (10:0.5 mg/kg; intramuscular injection) followed by propofol (1 ml/kg/h; intravenously). A midline incision was made on the dorsal surface of the skull extending to the cervical region and two bilateral craniotomies were performed with a burr. Two autostatic flexible Yasargil arms were installed on each side of the animal, using the Greenberg holder system (Codman). SmartFlow cannulas were secured at the tip of each flexible arm and inserted into each burr hole at a depth corresponding to the target areas of the *centrum ovale* (determined following MRI imaging from baseline anatomical MRI). Four infusions of 50 μL were administered into the white matter in each animal (two per hemisphere) at a flow rate of 5 μL/min (total dose of 7.2E+11 vg).

Gadolinium Distribution

Within 30 min after incision closure, animals were placed into the MRI scanner for coronal and sagittal imaging of the brain. MRI

images were uploaded to OsiriX MD. The gadolinium signal was manually outlined from sequential sections to determine the diffusion volume from each injection.

Necropsy and Sample Processing

Mice were humanely euthanized by slow-fill CO_2 asphyxiation at 17 or 30 weeks of age. Intra-cardiac punch was used to sample whole blood. Mice then underwent a 3-min intra-cardiac perfusion with 30 mL of PBS to remove blood from the organs. The organs were removed and weighed. Right brain hemispheres were fixed in 4% paraformaldehyde/PBS and left hemispheres were cut into five hemi-coronal, 2-mm slices. Slices 1, 3, and 5 were snap-frozen for biochemical analysis. Slices 2 and 4 were taken for qPCR/qRT-PCR evaluation.

Dogs were humanely euthanized 4 weeks after injection. Animals were transcardially flushed with cold 0.9% saline solution. Brains were cut into 3-mm-thick hemi-coronal slices. The even-numbered slabs were placed in sterile Petri dishes with the caudal side facing up and placed on ice. Eight-millimeter biopsy punches (up to 40 per hemisphere) were immediately taken and cut in half—one half for qPCR and one half for SGSH enzyme analysis. The odd-numbered slabs were placed in 4% paraformaldehyde and transferred to 30% sucrose 48 h after fixation. The tissue slabs were stored refrigerated (2°C–8°C).

NHPs were humanely euthanized 6 weeks after injection and transcardially flushed with cold 0.9% saline solution. The right and left hemispheres of the brain were cut into 4-mm-thick hemi-coronal slices in a dedicated primate matrix. The even-numbered slabs were placed in sterile Petri dishes with the caudal side facing up, placed on ice, and sliced into 10 × 10-mm squares (up to 53 per hemisphere). These were then cut in half—one half for qPCR and one for SGSH enzyme analysis. The odd-numbered slabs were placed in 4% paraformaldehyde and transferred to 30% sucrose 48 h after fixation. The tissue slabs were stored refrigerated (2°C–8°C).

SGSH Assay

SGSH activity in brain homogenates was measured using the fluorogenic substrate 4-methylumbelliferyl-α-D-*N*-glucosaminide (4MU-αGlcNS).[32] Results were expressed either as pmol/min/mg total protein compared to a 4MU standard curve (mouse homogenates) or as percentage of endogenous activity, determined as the mean value of 80 brain punches from two vehicle-injected hemispheres of two distinct animals for dogs or 85 punches from the two hemispheres of one PBS-injected animal for NHPs.

Vector Copy Number

Analysis of vector biodistribution was performed by quantitative TaqMan PCR (qPCR). Genomic DNA from brain homogenates was extracted using a NucleoSpin tissue kit (Macherey-Nagel). For quantification of AAV vector copy numbers, a standard curve was prepared by adding specific amounts of linearized LYS-SAF302 plasmids at a concentration of 2E+12 gc/mL. Quantification of endogenous gene β_2-microglobulin was used to monitor potential inhibitory effect of tissues on qPCR reaction. The primer sequences used to quantify AAV vector copy numbers were 5′-CCA GCC CCT CCA CAA TGA-3′ (forward), 3′-CAC TGG AGT GGC AAC TTC CA-5′ (reverse), and 5′-CAT CCC TGT GAC CCC-3′ (probe).

Results originally expressed as vector copy per μg of DNA were converted into vector copy per cell by considering genome median total length per cell of 2,254.63 Mb for *Canis lupus familiaris* and 2,946.84 Mb for *Macaca fascicularis*.

HS Analysis

Samples were prepared and mass spectrometric analysis of resulting disaccharides was performed as described in He et al.[54] using a modified gradient running from 1% mobile phase B (acetonitrile 0.1% formic acid) to 5% over 2 min, followed by a step to 20% and linear gradient to 25% over 3 min, followed by a 2.5-min wash step at 99% mobile phase B and then re-equilibration at 1% mobile phase B for 1 min. Disaccharide concentration was determined by relative peak area of a disaccharide GlcN-GlcUA α1-6 di butylated disaccharide (*m/z* 468.2/162.08) standard curve to a d9 deuterated analog internal standard (*m/z* 477.3/162.08), both synthesized by Assoc. Prof. Vito Ferro (University of Queensland, Australia).

Samples were run in a total of six batches. At each age after euthanasia, the batches were male slice 1, female slice 1, male slice 3, female slice 3, male slice 5, and female slice 5, and thus all dose groups/sex were run within a single batch. The inter-batch coefficient of variation (CV), calculated using quality control (QC) samples, was 9.2% for mice euthanized at 12 weeks post-injection and the intra-batch CV was <5.8%. For mice euthanized at 25 weeks post-injection, the inter-batch and intra-batch CVs were 11.9% and <12.2%, respectively.

GM2/GM3 Ganglioside Analysis

The most abundant species of GM2 and GM3 (d18:1/18:0) were quantified in the same brain slices using a previously published method.[55] All sample preparations and measurements were carried out by an experimenter blind to genotype/treatment. Samples were analyzed in a random order interspersed with blank injections of milliQ water. Samples were run in three batches, after each of two euthanasia times (i.e., six batches in total). The batches were slice 1, slice 3, and slice 5 at each euthanasia time. At 12 weeks post-injection, the inter-batch CV, calculated using three QC samples, was 27.2% for GM2 and 22.1% for GM3. The intra-batch CV was <26.9%. At the 30 weeks of age euthanasia time, the inter-batch CV, calculated using three QC samples, was 56% for GM2 and 66% for GM3. The intra-batch CV was <40%.

Immunohistochemistry and Histochemistry

Fixed brains were embedded in paraffin and sectioned at two levels (midline and at the injection site), with the level confirmed in H&E-stained sections prior to staining with antibodies and histochemical stains. Staining and analysis/quantification of disease-lesions were undertaken by a technician blinded to genotype and

treatment status. Samples were stained for the following markers: SGSH protein, LIMP-2 staining for endosomal/lysosomal system expansion, GFAP staining for activated astrocytes, isolectin B4 staining for activated microglia, and ubiquitin staining for axonal lesions as previously described.[19,56]

Serum Anti-SGSH and Anti-AAV Antibody Analysis

For mice, serum samples were assayed for the presence of anti-SGSH antibodies using a previously described horseradish peroxidase (HRP)-based assay.[57] To detect anti-AAV antibodies, Immulon 4HBX plates (Thermo Scientific #6404) were coated with AAVrh.10 particles and, after an overnight incubation (4°C), washed twice in wash buffer (0.25 M NaCl, 0.02 M Tris, pH 7.0). Blocking solution (wash buffer [0.25M NaCl, 0.02 M Tris, pH 7.0] containing 0.5% [w/v] gelatin and 0.2% [v/v] Tween 20) was added for 2 h before being replaced with serum samples diluted in blocking solution. After incubation at room temperature for 2 h, the plates were washed and a sheep anti-mouse HRP antibody (1:2,000; GE Healthcare #NA931) was added and incubated at room temperature for 1 h. Plates were washed and exposed to substrate (2,2′-azino-bis(3-ethylbenzothiazoline-6-sulfonic acid) diammonium salt; Sigma, catalog #A1888) on a shaker at room temperature for 20 min. The absorbance was read at 405 nm (1 s) on a Wallac Victor 1420 plate reader. Antibody titers are expressed as the lowest serum dilution giving an absorbance greater than two standard deviations above the blank.

For NHPs, serum samples were assayed for the presence of anti-SGSH antibodies using MaxiSorp 96-well microplates (Thermo Scientific #442404) coated with 10 ng/well of huSGSH (Abnova #H00006448-P01) and, after an overnight incubation (4°C), washed three times in 300 μL/well of wash buffer (PBS with 0.05% Tween 20). Blocking solution (PBS with 0.1% BSA) was added and plates were incubated overnight (4°C). Diluted serum samples were deposited (100 μL/well) and, after incubation at 37°C for 90 min, the plates were washed five times with 300 μL/well of wash buffer, and 100 μL/well of an HRP-labeled anti-monkey immunoglobulin (Ig) (Coger #MBS538736) was deposited before incubation at 37°C for 90 min. Microplates were washed five times with 300 μL/well of wash buffer, and 100 μL of HRP substrate was added per well. Microplates were incubated 15 min at room temperature in an obscured place, and 100 μL of H_2SO_4 was added to stop the enzymatic reaction. Microplates were read at 450 nm using a spectrophotometer (Thermo Fisher Scientific, Multiskan FC microplate). Antibody titers are expressed as the lowest serum dilution, giving an absorbance greater than three standard deviations above the blank. The detection of AAVrh.10 neutralizing factors was based on a previously described *in vitro* transduction inhibition assay.[58] Briefly, a permissive cell line, previously infected with adenovirus type 5, was transduced with a recombinant LacZ-AAVrh10 vector, pre-incubated with a range of six serum dilutions (1:10, $1:10^2$, $1:10^3$, $1:10^4$, $1:10^5$, and $1:10^6$). The efficiency of transduction was assessed by two independent operators using light microscopy, by scoring the intensity of blue precipitate formed from X-gal substrate by the LacZ-encoded β-galactosidase. The titer of neutralizing antibodies was defined as the last dilution that inhibited transduction as compared to the control without serum. Each assay was validated with a negative control (cell transduction in the absence of serum) and a positive control (cell transduction in the presence of a known positive serum pool).

Statistical Analysis

GraphPad Prism v7.0 was used for statistical analysis. Data are presented as either individual values or mean ± SEM. One-way ANOVA with *post hoc* Bonferroni testing was undertaken. $p \leq 0.05$ was regarded to be statistically significant.

SUPPLEMENTAL INFORMATION

Supplemental Information can be found online at https://doi.org/10.1016/j.omtm.2019.12.001.

AUTHOR CONTRIBUTIONS

M.H. and K.M.H. designed experiments, conducted formal data analysis, and wrote the manuscript. M.L.D., S.J.T., D.N., B.M.K., H.B., P.J.T., L.K.W., A.A.L, M.F.S., and C.G. conducted the experiments. J.A., X.M., L.G., and M.P. contributed to the protocol development and provided expertise on experimental approaches. R.L. contributed to interpretation of the results and wrote the manuscript. All authors contributed to the editing of the manuscript.

CONFLICTS OF INTEREST

M.H., X.M., L.G., M.P., and R.L. are full-time employees and hold equity in Lysogene.

ACKNOWLEDGMENTS

We thank Kimberley S. Gannon for participation in the design and implementation of these studies. We gratefully acknowledge the assistance of the staff in the WCHN Animal Facility. We thank the MPI research team and John Bringas for help in the dog study; Michel Zerah, Thomas Roujeau and the MIRCen team, especially Romina Aron Badin, for help in the NHP study; the Onco Design team, especially Sophie Champlot, for qPCR analysis, and Rahima Yousif, for anti-SGSH antibody assays in NHP sera; the Gene Therapy Immunology Core team for the detection of AAV neutralizing factors in NHP sera; Nathalie Cartier and Julie Lieb for advice; and Karen Aiach for continuous support and discussions. These studies were funded by grants from Lysogene, who was also involved in study design.

REFERENCES

1. Valstar, M.J., Neijs, S., Bruggenwirth, H.T., Olmer, R., Ruijter, G.J., Wevers, R.A., van Diggelen, O.P., Poorthuis, B.J., Halley, D.J., and Wijburg, F.A. (2010). Mucopolysaccharidosis type IIIA: clinical spectrum and genotype-phenotype correlations. Ann. Neurol. *68*, 876–887.

2. Héron, B., Mikaeloff, Y., Froissart, R., Caridade, G., Maire, I., Caillaud, C., Levade, T., Chabrol, B., Feillet, F., Ogier, H., et al. (2011). Incidence and natural history of mucopolysaccharidosis type III in France and comparison with United Kingdom and Greece. Am. J. Med. Genet. A. *155A*, 58–68.

3. de Ruijter, J., Valstar, M.J., and Wijburg, F.A. (2011). Mucopolysaccharidosis type III (Sanfilippo syndrome): emerging treatment strategies. Curr. Pharm. Biotechnol. *12*, 923–930.

4. Foust, K.D., Nurre, E., Montgomery, C.L., Hernandez, A., Chan, C.M., and Kaspar, B.K. (2009). Intravascular AAV9 preferentially targets neonatal neurons and adult astrocytes. Nat. Biotechnol. *27*, 59–65.

5. Deverman, B.E., Pravdo, P.L., Simpson, B.P., Kumar, S.R., Chan, K.Y., Banerjee, A., Wu, W.L., Yang, B., Huber, N., Pasca, S.P., and Gradinaru, V. (2016). Cre-dependent selection yields AAV variants for widespread gene transfer to the adult brain. Nat. Biotechnol. *34*, 204–209.

6. Gray, S.J., Matagne, V., Bachaboina, L., Yadav, S., Ojeda, S.R., and Samulski, R.J. (2011). Preclinical differences of intravascular AAV9 delivery to neurons and glia: a comparative study of adult mice and nonhuman primates. Mol. Ther. *19*, 1058–1069.

7. Samaranch, L., Salegio, E.A., San Sebastian, W., Kells, A.P., Foust, K.D., Bringas, J.R., Lamarre, C., Forsayeth, J., Kaspar, B.K., and Bankiewicz, K.S. (2012). Adeno-associated virus serotype 9 transduction in the central nervous system of nonhuman primates. Hum. Gene Ther. *23*, 382–389.

8. Hinderer, C., Bell, P., Vite, C.H., Louboutin, J.P., Grant, R., Bote, E., Yu, H., Pukenas, B., Hurst, R., and Wilson, J.M. (2014). Widespread gene transfer in the central nervous system of cynomolgus macaques following delivery of AAV9 into the cisterna magna. Mol. Ther. Methods Clin. Dev. *1*, 14051.

9. Hordeaux, J., Wang, Q., Katz, N., Buza, E.L., Bell, P., and Wilson, J.M. (2018). The Neurotropic properties of AAV-PHP.B are limited to C57BL/6J mice. Mol. Ther. *26*, 664–668.

10. Rosenberg, J.B., Sondhi, D., Rubin, D.G., Monette, S., Chen, A., Cram, S., De, B.P., Kaminsky, S.M., Sevin, C., Aubourg, P., and Crystal, R.G. (2014). Comparative efficacy and safety of multiple routes of direct CNS administration of adeno-associated virus gene transfer vector serotype rh.10 expressing the human arylsulfatase A cDNA to nonhuman primates. Hum. Gene Ther. Clin. Dev. *25*, 164–177.

11. Hocquemiller, M., Giersch, L., Audrain, M., Parker, S., and Cartier, N. (2016). Adeno-associated virus-based gene therapy for CNS diseases. Hum. Gene Ther. *27*, 478–496.

12. Hudry, E., and Vandenberghe, L.H. (2019). Therapeutic AAV gene transfer to the nervous system: a clinical reality. Neuron *102*, 263.

13. Winner, L.K., Beard, H., Hassiotis, S., Lau, A.A., Luck, A.J., Hopwood, J.J., and Hemsley, K.M. (2016). A preclinical study evaluating AAVrh10-based gene therapy for Sanfilippo syndrome. Hum. Gene Ther. *27*, 363–375.

14. Tardieu, M., Zérah, M., Husson, B., de Bournonville, S., Deiva, K., Adamsbaum, C., Vincent, F., Hocquemiller, M., Broissand, C., Furlan, V., et al. (2014). Intracerebral administration of adeno-associated viral vector serotype rh.10 carrying human *SGSH* and *SUMF1* cDNAs in children with mucopolysaccharidosis type IIIA disease: results of a phase I/II trial. Hum. Gene Ther. *25*, 506–516.

15. Gray, A.L., O'Leary, C., Liao, A., Agúndez, L., Youshani, A.S., Gleitz, H.F., Parker, H., Taylor, J.T., Danos, O., Hocquemiller, M., et al. (2019). An improved adeno-associated virus vector for neurological correction of the mouse model of mucopolysaccharidosis IIIA. Hum. Gene Ther. *30*, 1052–1066.

16. McGlynn, R., Dobrenis, K., and Walkley, S.U. (2004). Differential subcellular localization of cholesterol, gangliosides, and glycosaminoglycans in murine models of mucopolysaccharide storage disorders. J. Comp. Neurol. *480*, 415–426.

17. Beard, H., Hassiotis, S., Gai, W.P., Parkinson-Lawrence, E., Hopwood, J.J., and Hemsley, K.M. (2017). Axonal dystrophy in the brain of mice with Sanfilippo syndrome. Exp. Neurol. *295*, 243–255.

18. Archer, L.D., Langford-Smith, K.J., Bigger, B.W., and Fildes, J.E. (2014). Mucopolysaccharide diseases: a complex interplay between neuroinflammation, microglial activation and adaptive immunity. J. Inherit. Metab. Dis. *37*, 1–12.

19. Hemsley, K.M., Beard, H., King, B.M., and Hopwood, J.J. (2008). Effect of high dose, repeated intra-cerebrospinal fluid injection of sulphamidase on neuropathology in mucopolysaccharidosis type IIIA mice. Genes Brain Behav. *7*, 740–753.

20. Cearley, C.N., Vandenberghe, L.H., Parente, M.K., Carnish, E.R., Wilson, J.M., and Wolfe, J.H. (2008). Expanded repertoire of AAV vector serotypes mediate unique patterns of transduction in mouse brain. Mol. Ther. *16*, 1710–1718.

21. Swain, G.P., Prociuk, M., Bagel, J.H., O'Donnell, P., Berger, K., Drobatz, K., Gurda, B.L., Haskins, M.E., Sands, M.S., and Vite, C.H. (2014). Adeno-associated virus serotypes 9 and rh10 mediate strong neuronal transduction of the dog brain. Gene Ther. *21*, 28–36.

22. Tardieu, M., Zerah, M., Husson, B., de Bournonville, S., Deiva, K., Adamsbaum, C., Vincent, F., Hocquemiller, M., Broissand, C., Furlan, V., et al. (2014). Intracerebral administration of adeno-associated viral vector serotype rh.10 carrying human SGSH and SUMF1 cDNAs in children with mucopolysaccharidosis type IIIA disease: results of a phase I/II trial. Hum. Gene Ther. *25*, 506–516.

23. Sondhi, D., Johnson, L., De, B., Janda, K., Souweidane, M., Kaplitt, M., Kosofsky, B., Yohay, K., Ballon, D., Dyke, J., et al. (2012). Long-term expression and safety of administration of AAVrh.10hCLN2 to the brain of rats and nonhuman primates for the treatment of late infantile neuronal ceroid lipofuscinosis. Hum. Gene Ther. Methods *23*, 324–335.

24. Zerah, M., Piguet, F., Colle, M.A., Raoul, S., Deschamps, J.Y., Deniaud, J., Gautier, B., Toulgoat, F., Bieche, I., Laurendeau, I., et al. (2015). Intracerebral gene therapy using AAVrh.10-hARSA recombinant vector to treat patients with early-onset forms of metachromatic leukodystrophy: preclinical feasibility and safety assessments in non-human primates. Hum. Gene Ther. Clin. Dev. *26*, 113–124.

25. Fraldi, A., Biffi, A., Lombardi, A., Visigalli, I., Pepe, S., Settembre, C., Nusco, E., Auricchio, A., Naldini, L., Ballabio, A., and Cosma, M.P. (2007). SUMF1 enhances sulfatase activities in vivo in five sulfatase deficiencies. Biochem. J. *403*, 305–312.

26. Fu, H., Cataldi, M.P., Ware, T.A., Zaraspe, K., Meadows, A.S., Murrey, D.A., and McCarty, D.M. (2016). Functional correction of neurological and somatic disorders at later stages of disease in MPS IIIA mice by systemic scAAV9-hSGSH gene delivery. Mol. Ther. Methods Clin. Dev. *3*, 16036.

27. Haurigot, V., Marcó, S., Ribera, A., Garcia, M., Ruzo, A., Villacampa, P., Ayuso, E., Añor, S., Andaluz, A., Pineda, M., et al. (2013). Whole body correction of mucopolysaccharidosis IIIA by intracerebrospinal fluid gene therapy. J. Clin. Invest. *123*, 3254–3271.

28. King, B., Hassiotis, S., Rozaklis, T., Beard, H., Trim, P.J., Snel, M.F., Hopwood, J.J., and Hemsley, K.M. (2016). Low-dose, continuous enzyme replacement therapy ameliorates brain pathology in the neurodegenerative lysosomal disorder mucopolysaccharidosis type IIIA. J. Neurochem. *137*, 409–422.

29. Sorrentino, N.C., D'Orsi, L., Sambri, I., Nusco, E., Monaco, C., Spampanato, C., Polishchuk, E., Saccone, P., De Leonibus, E., Ballabio, A., and Fraldi, A. (2013). A highly secreted sulphamidase engineered to cross the blood-brain barrier corrects brain lesions of mice with mucopolysaccharidoses type IIIA. EMBO Mol. Med. *5*, 675–690.

30. Sergijenko, A., Langford-Smith, A., Liao, A.Y., Pickford, C.E., McDermott, J., Nowinski, G., Langford-Smith, K.J., Merry, C.L., Jones, S.A., Wraith, J.E., et al. (2013). Myeloid/microglial driven autologous hematopoietic stem cell gene therapy corrects a neuronopathic lysosomal disease. Mol. Ther. *21*, 1938–1949.

31. Hopwood, J.J., and Elliott, H. (1982). Diagnosis of Sanfilippo type A syndrome by estimation of sulfamidase activity using a radiolabelled tetrasaccharide substrate. Clin. Chim. Acta *123*, 241–250.

32. Karpova, E.A., Voznyi YaV, Keulemans, J.L., Hoogeveen, A.T., Winchester, B., Tsvetkova, I.V., and van Diggelen, O.P. (1996). A fluorimetric enzyme assay for the diagnosis of Sanfilippo disease type A (MPS IIIA). J. Inherit. Metab. Dis. *19*, 278–285.

33. Hinderer, C., Bell, P., Gurda, B.L., Wang, Q., Louboutin, J.P., Zhu, Y., Bagel, J., O'Donnell, P., Sikora, T., Ruane, T., et al. (2014). Intrathecal gene therapy corrects CNS pathology in a feline model of mucopolysaccharidosis I. Mol. Ther. *22*, 2018–2027.

34. Murrey, D.A., Naughton, B.J., Duncan, F.J., Meadows, A.S., Ware, T.A., Campbell, K.J., Bremer, W.G., Walker, C.M., Goodchild, L., Bolon, B., et al. (2014). Feasibility and safety of systemic rAAV9-hNAGLU delivery for treating mucopolysaccharidosis IIIB: toxicology, biodistribution, and immunological assessments in primates. Hum. Gene Ther. Clin. Dev. *25*, 72–84.

35. Hinderer, C., Katz, N., Buza, E.L., Dyer, C., Goode, T., Bell, P., Richman, L.K., and Wilson, J.M. (2018). Severe toxicity in nonhuman primates and piglets following high-dose intravenous administration of an adeno-associated virus vector expressing human SMN. Hum. Gene Ther. *29*, 285–298.

36. Rosenberg, J.B., Kaplitt, M.G., De, B.P., Chen, A., Flagiello, T., Salami, C., Pey, E., Zhao, L., Ricart Arbona, R.J., Monette, S., et al. (2018). AAVrh.10-mediated APOE2 central nervous system gene therapy for APOE4-associated Alzheimer's disease. Hum. Gene Ther. Clin. Dev. *29*, 24–47.

37. Hinderer, C., Bell, P., Katz, N., Vite, C.H., Louboutin, J.P., Bote, E., Yu, H., Zhu, Y., Casal, M.L., Bagel, J., et al. (2018). Evaluation of intrathecal routes of administration for adeno-associated viral vectors in large animals. Hum. Gene Ther. *29*, 15–24.

38. Bobo, R.H., Laske, D.W., Akbasak, A., Morrison, P.F., Dedrick, R.L., and Oldfield, E.H. (1994). Convection-enhanced delivery of macromolecules in the brain. Proc. Natl. Acad. Sci. USA *91*, 2076–2080.

39. Barua, N.U., Woolley, M., Bienemann, A.S., Johnson, D., Wyatt, M.J., Irving, C., Lewis, O., Castrique, E., and Gill, S.S. (2013). Convection-enhanced delivery of AAV2 in white matter—a novel method for gene delivery to cerebral cortex. J. Neurosci. Methods *220*, 1–8.

40. Lonser, R.R., Sarntinoranont, M., Morrison, P.F., and Oldfield, E.H. (2015). Convection-enhanced delivery to the central nervous system. J. Neurosurg. *122*, 697–706.

41. Salegio, E.A., Samaranch, L., Kells, A.P., Forsayeth, J., and Bankiewicz, K. (2012). Guided delivery of adeno-associated viral vectors into the primate brain. Adv. Drug Deliv. Rev. *64*, 598–604.

42. Cearley, C.N., and Wolfe, J.H. (2006). Transduction characteristics of adeno-associated virus vectors expressing cap serotypes 7, 8, 9, and Rh10 in the mouse brain. Mol. Ther. *13*, 528–537.

43. Skorupa, A.F., Fisher, K.J., Wilson, J.M., Parente, M.K., and Wolfe, J.H. (1999). Sustained production of β-glucuronidase from localized sites after AAV vector gene transfer results in widespread distribution of enzyme and reversal of lysosomal storage lesions in a large volume of brain in mucopolysaccharidosis VII mice. Exp. Neurol. *160*, 17–27.

44. Bosch, A., Perret, E., Desmaris, N., and Heard, J.M. (2000). Long-term and significant correction of brain lesions in adult mucopolysaccharidosis type VII mice using recombinant AAV vectors. Mol. Ther. *1*, 63–70.

45. Hennig, A.K., Levy, B., Ogilvie, J.M., Vogler, C.A., Galvin, N., Bassnett, S., and Sands, M.S. (2003). Intravitreal gene therapy reduces lysosomal storage in specific areas of the CNS in mucopolysaccharidosis VII mice. J. Neurosci. *23*, 3302–3307.

46. Luca, T., Givogri, M.I., Perani, L., Galbiati, F., Follenzi, A., Naldini, L., and Bongarzone, E.R. (2005). Axons mediate the distribution of arylsulfatase A within the mouse hippocampus upon gene delivery. Mol. Ther. *12*, 669–679.

47. Passini, M.A., Lee, E.B., Heuer, G.G., and Wolfe, J.H. (2002). Distribution of a lysosomal enzyme in the adult brain by axonal transport and by cells of the rostral migratory stream. J. Neurosci. *22*, 6437–6446.

48. Chen, F., Vitry, S., Hocquemiller, M., Desmaris, N., Ausseil, J., and Heard, J.M. (2006). alpha-L-Iduronidase transport in neurites. Mol. Genet. Metab. *87*, 349–358.

49. Neufeld, E.F. (1991). Lysosomal storage diseases. Annu. Rev. Biochem. *60*, 257–280.

50. Kornfeld, S. (1992). Structure and function of the mannose 6-phosphate/insulinlike growth factor II receptors. Annu. Rev. Biochem. *61*, 307–330.

51. Bielicki, J., Hopwood, J.J., Melville, E.L., and Anson, D.S. (1998). Recombinant human sulphamidase: expression, amplification, purification and characterization. Biochem. J. *329*, 145–150.

52. Crawley, A.C., Gliddon, B.L., Auclair, D., Brodie, S.L., Hirte, C., King, B.M., Fuller, M., Hemsley, K.M., and Hopwood, J.J. (2006). Characterization of a C57BL/6 congenic mouse strain of mucopolysaccharidosis type IIIA. Brain Res. *1104*, 1–17.

53. Paxinos, G., and Franklin, K.B.J. (2001). The Mouse Brain in Stereotaxic Coordinates (Academic Press).

54. He, Q.Q., Trim, P.J., Lau, A.A., King, B.M., Hopwood, J.J., Hemsley, K.M., Snel, M.F., and Ferro, V. (2019). Synthetic disaccharide standards enable quantitative analysis of stored heparan sulfate in MPS IIIA murine brain regions. ACS Chem. Neurosci. *10*, 3847–3858.

55. Marshall, N.R., Hassiotis, S., King, B., Rozaklis, T., Trim, P.J., Duplock, S.K., Winner, L.K., Beard, H., Snel, M.F., Jolly, R.D., et al. (2015). Delivery of therapeutic protein for prevention of neurodegenerative changes: comparison of different CSF-delivery methods. Exp. Neurol. *263*, 79–90.

56. Beard, H., Hassiotis, S., Luck, A.J., Rozaklis, T., Hopwood, J.J., and Hemsley, K.M. (2016). Continual low-dose infusion of sulfamidase is superior to intermittent high-dose delivery in ameliorating neuropathology in the MPS IIIA mouse brain. JIMD Rep. *29*, 59–68.

57. Hemsley, K.M., King, B., and Hopwood, J.J. (2007). Injection of recombinant human sulfamidase into the CSF via the cerebellomedullary cistern in MPS IIIA mice. Mol. Genet. Metab. *90*, 313–328.

58. Guilbaud, M., Devaux, M., Couzinié, C., Le Duff, J., Toromanoff, A., Vandamme, C., Jaulin, N., Gernoux, G., Larcher, T., Moullier, P., et al. (2019). Five years of successful inducible transgene expression following locoregional adeno-associated virus delivery in nonhuman primates with no detectable immunity. Hum. Gene Ther. *30*, 802–813.